SRTTU

JCARME
ISSN: 2228-7922
Journal of Computational and Applied Research in Mechanical Engineering
Vol. 8, No. 1, pp. 39-48
jcarme.sru.ac.ir

Analysis of deep drawing process to predict the forming severity considering inverse finite element and extended strain-based forming limit diagram

M. Bostan Shirin[a], R. Hashemi[b] and A. Assempour[c,*]

[a]School of biomedical Engineering, AmirKabir University of Technology, Tehran, Iran
[b]School of Mechanical Engineering, Iran University of Science and Technology, Tehran, Iran
[c]Center of Excellence in Design, Robotics and Automation, Department of Mechanical Engineering, Sharif University of Technology, Tehran, Iran.

Article info:
Received: 23/07/2016
Accepted: 10/01/2018
Online: 10/04/2018

Keywords:
Sheet metal forming,
Inverse finite element method,
Strain path,
Blank shape,
Nonlinear deformation,
Extended strain-based forming limit diagram.

Abstract
An enhanced unfolding inverse finite element method (IFEM) is used together with an extended strain-based forming limit diagram (EFLD) to develop a fast and reliable approach to predict the feasibility of the deep drawing process of a part and determining where the failure or defects can occur. In the developed unfolding IFEM, the meshed part is properly fold out on the flat sheet and treated as a 2D problem to reduce the computation time. The large deformation relations, nonlinear material behavior and friction conditions in the blank holder zone are also considered to improve the accuracy and capability of the proposed IFEM. The extended strain-based forming limit diagram based on the Marciniak and Kuczynski (M-K) model is computed and used to predict the onset of necking during sheet processing. The EFLD is built based on equivalent plastic strains and material flow direction at the end of forming. This new forming limit diagram is much less strain path dependent than the conventional forming limit diagram. Furthermore, the use and interpretation of this new diagram are easier than the stress-based forming limit diagram. Finally, two applied examples are presented to demonstrate the capability of the proposed approach.

Nomenclature

$\boldsymbol{\varepsilon}$	Strain components matrices
$\boldsymbol{\sigma}$	Stress components matrices
$\mathbf{a}$	Displacement vector
$\mathbf{T}$	Traction forces
E_{ij}	Green strain tensor components
$\mathbf{f}$	In-plane external force vector
r	Normal anisotropy factor
$Y(\bar{\varepsilon})$	Yield stress
$\bar{\sigma}$	Equivalent stress
$\bar{\varepsilon}$	Equivalent strain
ρ	Strain ratio

1. Introduction

Sheet metal forming is one of the most important production methods used in different industries such as producing industrial parts, office and

Corresponding author
email addresses: assem@sharif.edu

home appliances, automobile body, airplane parts, etc. [1]. As a whole system, the sheet metal forming consists of the feasibility study, process planning, die design, die manufacturing and stamping. In order to prevent failures in the trial out process and reduce design cost by predicting cracking and wrinkling tendencies, numerical simulations including finite element method (FEM) are applied to check part and die geometry at early design stage [2]. But many process parameters, such as die geometry, blank shape, sheet thickness, blank holding force and friction condition, affect the sheet deformation and it is well known that it is very important to choose an appropriate value of them to have a successful forming process. The commonly used forward finite element method (FEM), based on the incremental formulation, can consider these factors and simulate the process with high accuracy. However, in the forward method, computations start with the given process parameters that are unknown at the initial design stage. Therefore, trial and error is the nature of the forward method which is very time-consuming. For this reason, the necessity of some approaches arises to determine drawing feasibility quickly.

While designing the process of sheet metal forming, the designers consider more about how to rapidly calculate the blank shape and the thickness strain distribution from a given product model [3,4]. Therefore, different methods have been developed to estimate the blank shape which has different accuracies. There have been several attempts to design the blank shape and estimate the strain distribution in a deformed part with deformation theory of plasticity. It has been shown that these methods have the best accuracy. Majlessi and Lee [5, 6] showed that using this theory is reasonable for rapid simulation in the first stage of design. They extended the theory of Levy et al. [7] and applied it to axisymmetric one step and multi-stage problems, obtaining good results. However, this method cannot be applied without considering boundary conditions like friction and blank holder force. Therefore, the crash form process cannot be analyzed by this approach. Guo and Batoz [8, 9] used virtual work theory and derived a formulation for field problems as an inverse method to obtain the initial blank shape and the thickness distribution in a deformed part. Although their method does not need to have initial boundary conditions, its accuracy reduces the simulation of parts with vertical walls. The mentioned methods considered the problem in the 3-D coordinate system and used nonlinear strain-stress relations that have to be solved numerically; as a result, they required high computation cost and their convergence depends on the appropriate selection of the initial guess.

Based on the work of Liu and Karima [10], Assempour et al. [11-13] proposed a one-step inverse finite element method (IFEM), known as unfolding technique. Their formulations are based on the infinitesimal strain relations and the principle of potential energy minimization. In their method, the 3D problem is unfolded on the flat sheet and therefore, treated as 2D one. Their formulation ends to a linear system of equations which can be easily solved without convergence problems involved in nonlinear methods. This method is very efficient and fast in obtaining the initial blank shape and size. Although due to the nature of linear formulations, the strain values are less accurate compared with the nonlinear IFEM approaches, they have shown that the results accuracy is acceptable, and it is logical to use their method because it is too fast and its convergence is guaranteed.

The calculated strain distribution can be used in forming limit diagrams (FLD) to determine how close the sheet metal is to tearing when it is formed to a product shape [14]. The forming limit diagram is used in sheet metal forming analysis to predict how the sheet metal is close to the necking point. The strain-path dependent nature of the forming limit diagram (FLD) causes the method to become ineffective in the analysis of complex sheet metal forming processes [15, 16]. Recently, the experimental and theoretical results showed that the extended strain-based forming limit diagram is less sensitive to the strain path effect than the FLD (e.g., see [17]).

According to above reviews, IFEM is a powerful tool in the industry and very useful in the early design stage to predict the initial blank shape and decrease the computation cost by eliminating trial and errors for blank shape

estimation. Moreover, it can help to check drawing feasibility if combined with FLD. So the more precise the results, the better the prediction is obtained.

This paper presents a combination of two techniques: (1) an inverse finite element analysis to predict strains in a formed part and (2) the "extended" forming limit diagram which plots forming limits in terms of effective strain versus strain path [18], and thus provides a forming evaluation that is not nearly as sensitive to strain path as the conventional forming limit diagram. This combination of technologies is very applicable to deep drawing parts since such parts typically exhibit significantly non-linear loading.

In this paper, an enhanced unfolding IFEM is introduced. Green strain relations and material hardening are used for the fast calculation of strain distribution, and the extended strain-based forming limit diagram based on the Marciniak and Kuczynski (M-K) model [16] is computed and used for exploring forming severity. The extended strain-based forming limit diagram is used for investigation of the process [19]. The extended strain-based forming limit diagram is built based on equivalent plastic strains and material flow direction at the end of forming. This new forming limit diagram is much less strain path dependent than the conventional forming limit diagram. Furthermore, the use and interpretation of this new diagram is easier than the stress-based forming limit diagram. Finally, two applied examples are simulated by the proposed method and forming severity, and their drawing feasibility are investigated.

2. Unfolding inverse finite element formulations

IFEM determines the initial blank shape as well as strain distribution in a given deformed 3D part (final part). Assumptions made in this method are as follows:

(a) material hardening law with normal anisotropy; (b) plane stress condition; (c) deformation theory of plasticity and (d) material with the rigid-plastic model.

The formulations relate the initial state of the material points on the flat sheet to their final state on the given part. In the inverse problem, the geometry of the final part and the thickness of the initial blank sheet, are given while the unknowns are the nodal coordinates on the flat sheet and the thickness distribution on the final part.

As the geometry of the 3D part is given, the vertical movement of material is known, and the only unknown is the displacements in the horizontal plane. In the unfolding technique, the geometry of the 3D part is discretized by the membrane elements, and all of them are properly unfolded on the flat sheet to convert the 3D problem to 2D one. In this technique, as it is displayed in Fig. 1, each element is rotated about a given axis until its normal vector becomes parallel to the global z-axis [12].

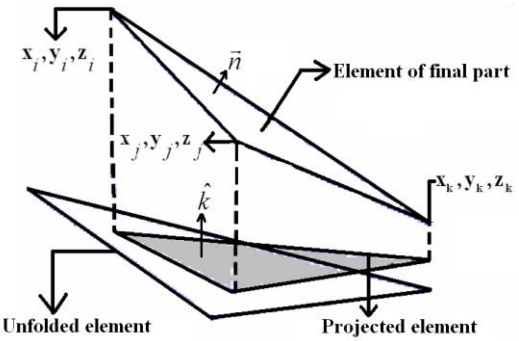

Fig. 1. Projection and unfolding process for an element of final part.

The nodal coordinates of projected elements on the flat sheet are used as initial guess for the nodal positions in the initial configuration. The coordinates of the initial nodal position are then improved over the computations by applying the principle of the minimum potential energy.

The first version of unfolding technique was based on the linear finite element formulations; after that, nonlinear deformation relations have been implemented in this technique to improve its accuracy [20].

The increment of potential energy (W) in a deformed body is:

$$\delta W = \int_V \delta \boldsymbol{\varepsilon}^T \boldsymbol{\sigma} \, dV - \int_S \mathbf{a}^T \mathbf{T} \, dS \qquad (1)$$

In the drawing process, material points undergo finite strains and therefore the Green strain tensor is the appropriate form for strain measure:

$$\mathrm{E}_{ij} = \frac{1}{2}\left(u_{i,j} + u_{j,i} + u_{k,i}u_{k,j}\right) \quad (2)$$

It is possible to express the Green strain tensor as the product of a nonlinear operator with the nodal displacement of the element as follows:

$$\mathbf{E}^e = \mathbf{B}\mathbf{a}^e \quad (3)$$

where $\mathbf{B}$ is the nonlinear strain operator [21]. $\mathbf{B}$ depends on the derivative of the displacement field; therefore, it is dependent on the unknown nodal displacements. By differentiating Eq. (3) and substituting it in Eq. (1), the following relation is obtained:

$$\delta W = \int_V \mathbf{a}^T \mathbf{B}^T \boldsymbol{\sigma}\, dV - \int_S \mathbf{a}^T \mathbf{T}\, dS \quad (4)$$

A deformable body in a state of mechanical equilibrium state must satisfy the principle of virtual work as the necessary and sufficient condition for the stress field. Therefore, the first variation of the potential energy with respect to the unknown nodal displacements must vanish:

$$\frac{\delta W}{\delta \mathbf{a}} = \sum_{e=1}^{n} \int_{V^e} \mathbf{B}^T \boldsymbol{\sigma}^e\, dV^e - \sum_{e=1}^{n} \int_{S^e} \mathbf{T}\, dS^e = \sum_{e=1}^{n} \int_{V^e} \mathbf{B}^T \boldsymbol{\sigma}^e\, dV^e - \mathbf{f} = 0 \quad (5)$$

where $\mathbf{f}$ corresponds to the in-plane external forces to create the unknown nodal displacements. The calculations of the external forces are expressed in [21]. After discretization of the part and the integration over the all elements, Eq. (5) can be expressed as:

$$\sum_{e=1}^{n} \mathbf{B}^T \boldsymbol{\sigma}^e t^e \Delta - \sum_{e=1}^{n} \mathbf{f}^e = 0 \quad (6)$$

The stress components matrix can be expressed in terms of strain components matrix using the stress-strain relationship of the material. Hill's criterion for anisotropic materials under plane stress condition has been used to evaluate this function [22]:

$$f = \left(\boldsymbol{\sigma}^T \mathbf{P} \boldsymbol{\sigma}\right)^{0.5} - Y(\bar{\varepsilon}) = 0 \quad (7)$$

where

$$\mathbf{P} = \begin{bmatrix} 1 & -\frac{r}{1+r} & 0 \\ -\frac{r}{1+r} & 1 & 0 \\ 0 & 0 & 3 \end{bmatrix}$$

Using this criterion in the flow rule and adopting Hencky deformation theory of plasticity lead to the following result:

$$\boldsymbol{\sigma} = \frac{\bar{\sigma}}{\bar{\varepsilon}} \mathbf{P}\boldsymbol{\varepsilon} \quad (8)$$

Equivalent stress is calculated using Von Mises criteria and the equivalent strain is calculated using Hill's yield criterion [22] as follows:

$$\bar{\varepsilon} = \sqrt{\frac{2}{3}\frac{2+r}{1+2r}} \left[\begin{array}{l} (1+r)\varepsilon_x^2 + (1+r)\varepsilon_y^2 \\ \qquad + 2r\varepsilon_x \varepsilon_y + 0.5\gamma_{xy}^2 \end{array} \right]^{1/2} \quad (9)$$

Substituting Eq. (8) in Eq. (6) results in the following nonlinear equation:

$$\sum_{e=1}^{n} \mathbf{B}^T \left(\frac{\bar{\sigma}}{\bar{\varepsilon}}\right) \mathbf{P}^{-1} \mathbf{B}\mathbf{a} A^e t^e - \sum_{e=1}^{n} \mathbf{f}^{\mathbf{e}} = 0 \quad (10)$$

Nodal displacements ($\mathbf{a}$) can be obtained by solving the above system of equations, using the Newton-Raphson method.

3. The extended strain-based forming limit diagram

As mentioned earlier, the FLD is strain path dependent. So this curve cannot be applied to analyze sheet metal forming process taken under non-linear strain paths. However, an extended strain-based forming limit curve is presented, and this diagram is much less sensitive to strain path changes than the conventional FLD. This extended strain-based FLD is constructed based on effective strains (equivalent strains) at the onset of localized necking and material flow direction at the end of sheet metal forming (Table 1) [16, 17]. In this work, the extended strain-based forming limit diagram based on the

Marciniak and Kuczynski (M-K) model is computed and used to predict the onset of necking during sheet processing.
The current strain path ρ is defined as the ratio of the incremental minor strain to the major strain and is expressed as follows:

$$\rho = \frac{d\varepsilon_2}{d\varepsilon_1} \tag{11}$$

By using a yield function and an associated flow rule, the strain ratio ρ can be related to the stress ratio σ_2/σ_1.

The extended strain-based FLD can be used to specify part quality in the press shop by measuring the principal surface strains in areas of concern. Then the strain ratios and the equivalent strain at the determined locations can be calculated (e.g., from Eqs. 10 and 11). The forming process would be safe if all the measured effective strains are located under the extended strain-based FLD. The proposed method and steps of part analysis are shown in the flowchart of Fig. 2.

Table 1. The comparison between different FLD criteria [16].

Criterion	Advantages	Disadvantages
Forming limit diagram	Cool analysis FLD extensively applied to evaluate localized necking in shee metal forming process because of its straight-forwardness and suitability of measuring deformation strains either practically in forming tests or simulatively in finite element simulation	Subtle to strain path variations
Forming limit stress diagram (FLSD)	FLSD has the benefit of not depending on strain paths FLSD be able to be suitably converted from conventional strain-based FLD	Limited applications in industrial practice
Extended strain-based forming limit diagram (EFLD)	EFLD has the benefit of not depending on strain paths The use and interpretation of EFLD is easier than FLSD	-

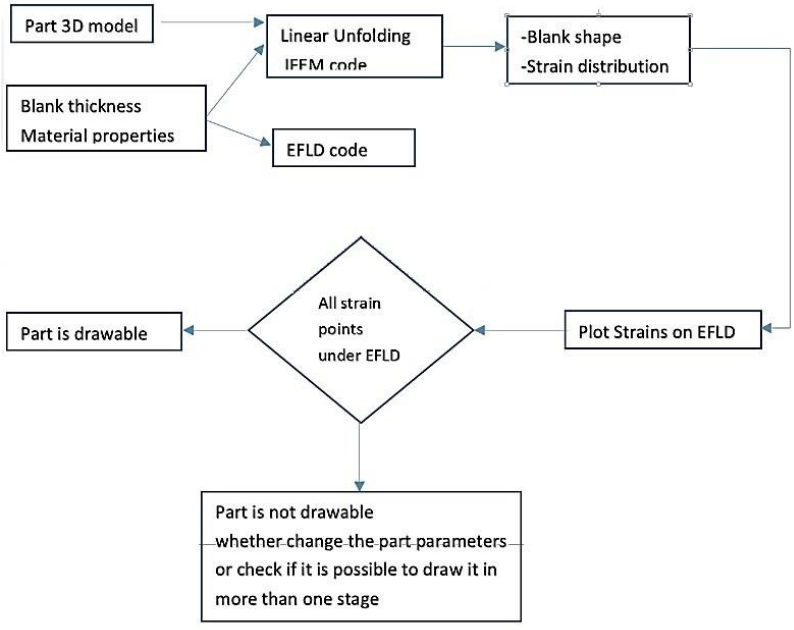

Fig. 2. Flowchart of using IFEM together with EFLD to predict drawing feasibility.

4. Results and discussion

The inverse algorithm and FLD are implemented in a finite element code and applied to several examples in sheet metal forming. Among them, two applied examples, including junction box and compressor housing, are selected for discussions and confirmations of the method.

4.1. Junction box example

The Junction box is a square part of $177\,mm$ and $24mm$ sides and corner radii, respectively. The part is $127\,mm$ deep and has a flange of $6mm$. The punch and die profile radii are $5mm$ and the part is drawn from a $2mm$ sheet of steel. The material properties of this part are as follows:

$$Stress-Strain\ behavior \quad \bar{\sigma}=551\bar{\varepsilon}^{n}\ MPa$$

$$Normal\ anisotropy\ factor \quad r=0.8$$

The minimum rectangular blank size used in industry is $411mm\times411mm$ which its forming is very difficult, and it is very sensitive to the process parameters [23].

Because of the symmetry condition, only a quarter of the part is modeled. The final part is meshed by 2084 elements and analyzed by the developed inverse method. Figs. 3 and 4 show the calculated blank shape and thickness strain distribution on the proposed part, respectively.

Fig. 4 shows that strain in punch and die radius zones is high, and rupture or wrinkling can occur in these sections. To verify the accuracy of the obtained strain distribution, the forward simulation is done with the obtained blank shape in ABAQUS explicit. Fig. 5 shows the obtained part and its thickness strain distribution from forwarding simulation. It is obvious that the drawn part is near to the desired junction box and its flange zone is similar the desired part. Moreover, it shows that the high strain zones are the same as predicted by IFEM.

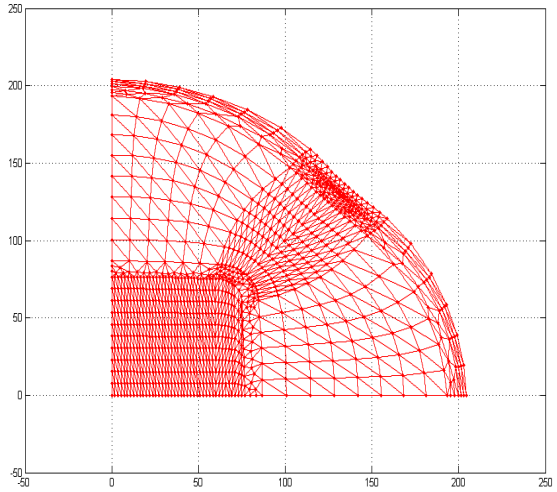

Fig. 3. Blank shape calculated by the developed IFEM.

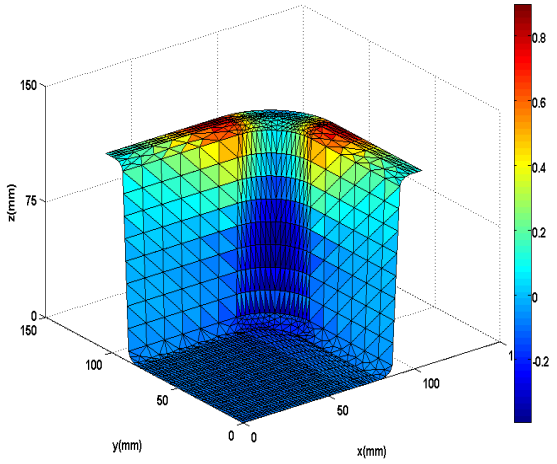

Fig. 4. Thickness strain distribution calculated by the developed IFEM.

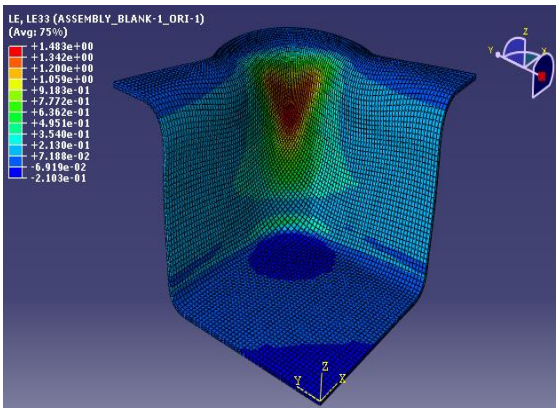

Fig. 5. The obtained part from drawing simulation in ABAQUS explicit**.**

The trial and error step for blank shape and size determination is omitted, and part displayed in Fig. 5 is obtained in the first simulation run. The thickness strain along the side of the part calculated by the inverse approach and forward method is compared in Fig. 5. To show the effect of implementing large deformation relations (Green strain) and material nonlinearity, the part is simulated with linear unfolding IFEM too, and the thickness strain distribution along the side is plotted in Fig. 5.

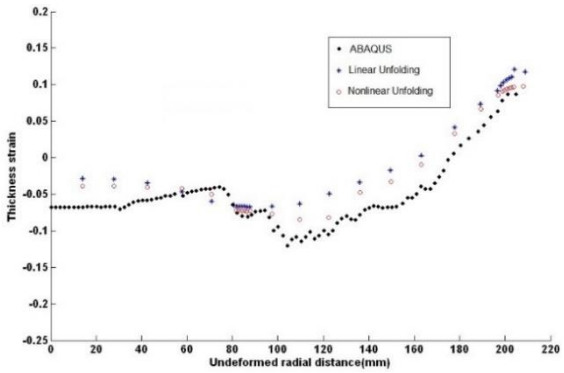

Fig. 6. Thickness strain along the junction box side.

It is clear that the results of the inverse method have the same trend as the forward simulation does, and they are more precise than the linear method. The maximum calculated error between the ABAQUS results and the linear unfolding IFEM and the nonlinear unfolding IFEM is 45% and 34%, respectively. It should be mentioned that because of using deformation theory of plasticity, inverse methods are not highly accurate tools for strain prediction in the part but it is possible to improve them to reduce the error. If the error is high, it cannot be used in FLD to predict drawing feasibility. The CPU time used for the nonlinear and linear unfolding IFEM method is 135S and 60S, respectively. Although the CPU time increased in the proposed method, it is too faster than the conventional inverse and the forward incremental methods. Therefore, the predicted strain distribution can be used in EFLD. Fig. 7 shows the calculated strains in the EFLD for the considered part.

All strains are below the EFLD and it can be concluded that this part can be drawn. According to deep drawing handbooks, this part can be manufactured by deep drawing, but it is difficult. It is observed the strains are too close to the rupture limit line and as it was reported in industry, forming of this part is very severe. So, it is observed that the nonlinear IFEM together with EFLD has predicted the severity and feasibility of the drawing.

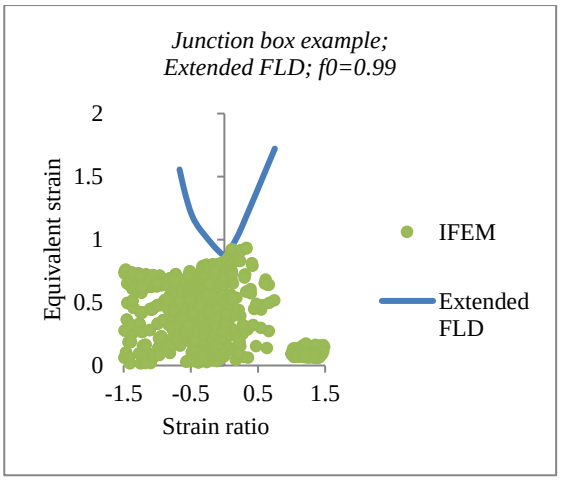

Fig. 7. Strain distribution plotted in the extended strain-based forming limit diagram (Junction box example)

4.2. Compressor housing example

To show the applicability of the proposed method in predicting the forming feasibility, a compressor housing is studied in this example. The geometry and material properties of this part are chosen as the ones reported in [24]. This part splits in the forming process, and it is not possible to form it with this process parameter. Fig. 8 shows the geometry parameters of the housing and the ruptured part. The material properties of this part are as follows:

$$Stress-Strain\,behavior \quad \bar{\sigma} = 612.9\bar{\varepsilon}^{0.209}\ MPa$$

$$Normal\ anisotropy factor \quad r = 0.95$$

The desired part is modeled and meshed with 2532 elements and analyzed by IFEM. Then the calculated strain distribution is plotted on the extended strain-based forming limit diagram. Figs. 9 and 10 show the EFLD plot and thickness strain distribution on the part, respectively. Regarding Fig. 8, some strain points are above the EFLD line which means that the part will be ruptured in the drawing

process and it is impossible to draw it. The elements whose strains are above the FLD are marked in Fig. 9. It is clear that the predicted rupturing zone is the same as the experimental tests shown in Fig. 7. It is observed that the method is also predicted rupturing in the considered part.

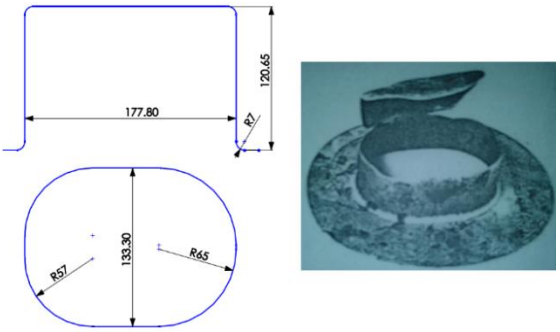

Fig. 8. Geometry of Compressor Housing and the ruptured part, dimensions are in millimeters.

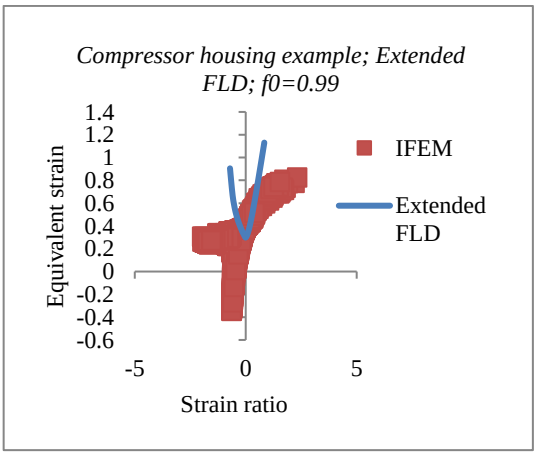

Fig. 9. Strain distribution plotted in the extended strain-based forming limit diagram (compressor housing example).

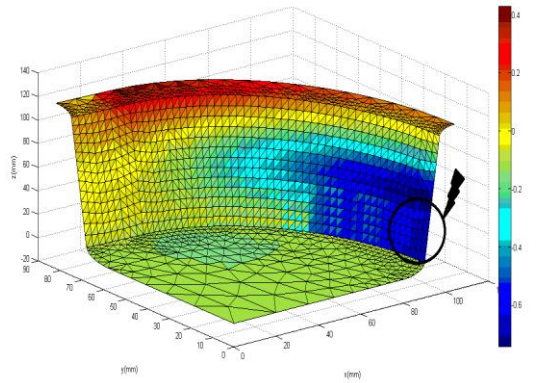

Fig. 10. Thickness strain distribution on the compressor housing example.

5. Conclusions

A quick and reliable method is introduced to predict the drawing process feasibility. To estimate the strain distribution on the concept part, an enhanced unfolding IFEM is developed. The blank shape and strain distributions are computed based on the potential energy minimization for the unfolded elements. To improve the accuracy of the method and to close to real condition, the Green-Lagrange strains is considered, and nonlinear plastic properties of the material are implemented in the numerical solution of the equation system. As a result, the proposed method has the advantage of low computation cost of linear unfolding IFEM and more precise results. To predict the drawing feasibility of the part, an extended strain-based FLD is used. This new FLD is much less strain path dependent than the conventional FLD. Finally, two applied examples are studied to show the utility of the method. First, the junction box is analyzed as a critical part of forming. The results show that maximum error between ABAQUS and inverse method is 45% for linear and 34% for nonlinear IFEM. So, the unfolding IFEM method is more accurate, and its result on the extended FLD is more reliable. The second example is the compressor housing as a part that is reported cannot be deep drawn with the desired process parameters. The method predicts both conditions very good. Therefore, the method can be used in the initial design stage to check drawability of the part and predicting the sections which are more probable to rupture.

Acknowledgment

The authors would like to acknowledge Iran National Science Foundation (INSF) for financing this research.

References

[1] Y. Liu, X. Peng, Y. Qin, “FE simulation for concurrent design and manufacture of automotive sheet-metal parts”, *Journal of Materials Processing Technology*, Vol. 150, No. (1-2), pp. 145-150, (2004).

[2] A. R. Joshi, K. D. Kothari, R. L. Jhala, "Effects Of Different Parameters On Deep Drawing Process: Review", *International Journal of Engineering Research & Technology*, Vol. 2, No. 3, pp. 1-5, (2013).

[3] X. Shi, J. Chen, Y. et al Peng, "A new approach of die shape optimization for sheet metal forming processes", *Journal of Materials Processing Technology*, Vol. 152, No. 1, pp. 35-42, (2004).

[4] J. Lan, X. Dong, Z. Li, "Inverse finite element approach and its application in sheet metal forming", *Journal of Materials Processing Technology*, Vol. 170, No. 3, pp. 624-631, (2005).

[5] S. A. Majlessi, D. Lee, "Deep drawing of square-shaped, sheet metal parts Part1", FEM, *Transaction of ASME*, Vol. 115,102-109, (1993).

[6] S. A. Majlessi, D. Lee, "Further development of sheet metal forming analysis method" *Transaction of the ASME*, Vol. 109, pp. 330-337, (1987).

[7] S. Levy, C. F. Shinh, J. P. D., et al., Wilkinson, "Analysis of sheet metal forming to axisymmetric shapes. In", *Formability Topics-Metallic Materials ASTM* (eds B A Niemeier, A K Schmeider, J R Newby), Toronto, Canada, pp. 238, (1978).

[8] J. L. Batoz, Y. Guo, F. Mercier, "The inverse approach with simple triangular shell elements for large strain predictions of sheet metal forming parts" *Eng. Comp*. Vol. 15, pp. 864-892, (1998).

[9] Y. Q. Guo, J. L. Batoz, "Recent developments on the analysis and optimum design of sheet metal forming parts using a simplified inverse approach", *Computers and Structures*, Vol. 78, No. (1-3) pp. 133-48, (2000).

[10] S. D. Liu, M. A. Karima, "One step finite element approach for production design of sheet metal stamping. In", *NUMIFORM 92* (eds J. L. Chenot, R. D. Wood, O. C. Zienkiewicz), Valbonne, France. Rotterdam: A.A. Balkema, pp. 497-502, (1992).

[11] R. Azizi, A. Assempour, "Application of linear inverse finite element method in prediction of the optimum blank in sheet metal forming" *Materials and Design*, Vol. 29, No. 3, pp. 1965-72, (2008).

[12] F. M. Kankarani, M. Bostan shirin, A. Assempour, "Development of an inverse finite element method with an initial guess of linear unfolding", *Finite Element in Analysis and Design*, Vol. 79, pp. 1-8, (2014).

[13] M. Einolghozati, M. Bostan Shirin, A. Assempour, "Application of Inverse Finite Element Method in tube hydro forming modeling", *Applied Mathematical Modelling*, Vol. 37, No. 8, pp. 5913-5926, (2013).

[14] R. Hashemi, K. Abrinia, "Analysis of the extended stress-based forming limit curve considering the effects of strain path and through-thickness normal stress", *Materials and Design*, Vol. 54, pp. 670-677, (2014).

[15] A. Assempour, R. Hashemi, K. Abrinia, M. Ganjiani, E. Masoumi, "A methodology for prediction of forming limit stress diagrams considering the strain path effect", *Computational materials science*, Vol.45, No. 2, pp. 195-204, (2009).

[16] R. Hashemi, K. Abrinia, G. Faraji, "A methodology for determination of extended strain-based forming limit curve considering the effects of strain path and normal stress. Proceedings of the Institution of Mechanical Engineers, Part C", *Journal of Mechanical Engineering Science*, Vol. 229, No. 9, pp. 1537-1547, (2015).

[17] M. Nurcheshmeh, D. E. Green, "On the use of effective limit strains to evaluate the forming severity of sheet metal parts after nonlinear loading", *International Journal of Material Forming*, Vol. 7, pp. 1-18, (2014).

[18] N. Boudeau, J. C. Gelin, "Necking in sheet metal forming Influence of macroscopic and microscopic properties of materials", *International Journal of*

Mechanical Sciences, Vol. 42, No. 11, pp. 2209-2232, (2014).

[19] N. Boudeau, J. C. Gelin, "Post-processing of finite element results and prediction of the localized necking in sheet metal forming", *Journal of Materials Processing Technology*, Vol. 60, No. (1-4), pp. 325-330, (1996).

[20] M. Bostan shirin, A. Assempour, "Some improvements on the unfolding inverse finite element method for simulation of deep drawing process", *The International Journal of Advanced Manufacturing Technology*, Vol. 72, No. 1, pp. 447-456, (2014).

[21] A. Khoei, *Computational Plasticity in Powder Forming Processes*, 1st Edition, Elsevier, (2005).

[22] R. A. Hill, "Theory of the yielding and plastic flow of anisotropic metals", *Proc. R SocLond A.*, Vol. 193, pp. 281-297, (1948).

[23] A. Assempoor, M. Karima, "Interaction of Part Geometry and Material Properties with Forming Severity and Tooling Design for Box-Shaped Stampings, *SAE. International Congress* Detroit, Michigan, Feb. pp. 105-113, (1992).

[24] A. Assempoor, "Simulation of forming severity and blank development in general box-shaped parts", *International conference on engineering applications of mechanics*, Tehran, Iran, June, pp. 531-538, (1992).

How to cite this paper:
M. Bostan Shirin, R. Hashemi, A. Assempour, "Analysis of deep drawing process to predict the forming severity considering inverse finite element and extended strain-based forming limit diagram" *Journal of Computational and Applied Research in Mechanical Engineering*, Vol. 8, No. 1, pp. 39-48, (2018).

DOI: 10.22061/JTE.2018.2921.1740

URL: http://jte.sru.ac.ir/?_action=showPDF&article=778